The conical bore in musical acoustics

R. Dean Ayers, Lowell J. Eliason, and Daniel Mahgerefteh[a)]
Department of Physics–Astronomy, California State University at Long Beach, Long Beach, California 90840

(Received 9 April 1984; accepted for publication 18 May 1984)

A survey of descriptive textbooks on musical acoustics shows a need for a legitimate, convincing explanation for the seemingly paradoxical behavior of the conical bore. We examine the differential equations and their solutions for spherically symmetric waves in three dimensions, settling on acoustic pressure as the variable of interest because it behaves more simply than particle velocity or displacement. Next we solve the boundary-value problem for all combinations of open and closed ends on truncated cones. The natural frequencies so obtained are then justified with plots of the pressure standing waves; it is at this point that we find a physically correct explanation that can be shared with students in a descriptive acoustics course. This pictorial approach is also used to explain the shapes of the input impedance curves for a straight pipe and a frustum. We conclude with a careful analysis of the successive distortions to which a pressure pulse is subjected as it bounces back and forth inside a frustum.

I. BACKGROUND

The cone is an important basic bore shape for wind instruments, serving in a relatively pure form for the oboe, bassoon, and saxophone. Some conical early instruments are the shawn, dulcian, cornetto, and serpent. The Hebrew shofar, the Hungarian tarogato, and the Scottish bagpipe chanter are a few examples of the many folk instruments that employ conical bores. The shofar and the cornetto illustrate clearly the derivation of this bore shape from its natural occurrence in animal horns.

Two other simple geometries also serve as basic bore shapes: the open pipe (open at both ends) and the closed pipe (closed at one end only). The first of these is found in the flute, recorder, and most flue organ pipes. The closed pipe is represented by the clarinet, slide whistle, panpipes, bagpipe drones, krummhorn, racket, chalumeau, and stopped organ pipes.

These three simple shapes are all musically useful for the same reason: the frequencies of their various standing waves are members of a harmonic series. This is also the case for the more sophisticated mixtures of closed pipe and cone plus flaring bell used as the bores for all modern brass instruments, except that the fundamental or lowest mode's participation in the harmonic series is sacrificed. This relationship is important for the establishment of clear, well-centered (stable) notes via the feedback from the bore to a nonlinear driver. The alignment of higher bore resonances with the harmonics of the note being played helps to establish a strong, stable "regime of oscillation" or cooperative feedback condition among the components of the sound spectrum and the bore resonances.[1]

The open pipe has a fundamental wavelength that is twice the effective length of the pipe, including small, positive corrections at the two open ends, and it sounds all harmonics of the fundamental frequency. This is easily seen from graphs of the standing waves, like those at the top of Fig. 4, plotted either in terms of pressure variations as shown there or in terms of particle velocity (or displacement). The two types of graph are complements of each other: a pressure antinode is a velocity node, and a pressure node is a velocity antinode for these *planar* standing waves. Similar diagrams can be used to show that the closed pipe has a fundamental wavelength that is four times the effective pipe length, now with only one open-end correction, and that it sounds only the odd harmonics of its fundamental frequency. The observed behavior of the complete cone is the same as that of the open pipe; its fundamental wavelength is twice the cone's length, and all harmonics are sounded.

Casual examination of the conical bore might lead one to expect behavior identical with that of the *closed* pipe, since it is obviously closed at its apex. Even when a small portion is removed near the apex to make a useful instrument bore, the driver that is attached there functions as a closed end of the bore, forcing a pressure antinode and a velocity node at that end. Accurate plots of the standing waves for the closed pipe and the cone do bear a superficial resemblance to each other, because they satisfy identical boundary conditions at their corresponding ends. The resolution of this seeming paradox lies in the fact that the waves in a cone are spherical, while those in a pipe are planar. Unfortunately, books likely to be used in a descriptive musical acoustics course do not handle this situation at all adequately, and there is even some confusion about conical bores in the research literature.

II. THE STUDENT'S-EYE VIEW

Our survey of 14 textbooks and references on musical acoustics found four of these sources[2–5] taking the prudent course of simply stating the basic facts about the cone's behavior without pointing up the apparent paradox or venturing any explanation. Rigden[6] goes into considerable detail about the effects of truncation and discusses a specific numerical example, but he does not tell the reader how he did his calculations or attempt to make any physical explanation for what he finds. The full extent of Askill's treatment[7] is the statement that an *open* conical pipe has the same resonant frequencies as an open cylindrical pipe. This statement is true, but its connection with the behavior of a cone closed at its small end is not immediately apparent. Berg and Stork[8] give an equally brief (but highly erroneous) statement that "*any* section of a cone will resonate in the same basic manner as an open tube of approximately the same length, *even if one end of the cone is a reed end*" (our italics).

White and White[9] show accurate pressure standing

 © 1985 American Association of Physics Teachers

waves for the second modes in a complete cone and in an open pipe of the same length, like those at the bottom and the top of our Fig. 4, but they attempt to explain the conical standing waves in terms of those for a *closed* pipe. They state explicitly that the cone contains odd-integral numbers of quarter-wavelengths, but the varying diameter "distorts the wave shape so that the wave shape is stretched out in the narrow end and compressed in the widening end"—the clear (and false) implication being that the wave velocity increases as the bore narrows. This misguided effort is directed entirely at the shapes of the standing waves and yields no quantitative results for their frequencies. Taylor[10] uses a different approach, attempting to follow a pressure pulse as it reflects at each end of the cone. Whereas White and White need a higher wave velocity in the narrower portion of the cone, Taylor claims that "because the pipe has shrunk to a very small bore, the speed of the wave *slows down* and no real reflection occurs. Whether the end is open or closed, the wave is effectively *damped out*" (our italics). Taylor's argument, far from yielding the correct modal frequencies, actually implies that the cone will have no resonances.

Fletcher's slim volume[11] is written not as a self-contained textbook but as a supplement for a standard physics course. He acknowledges the seeming paradox explicitly and points out that its resolution lies in dealing with spherical waves. Unfortunately his plots of the standing waves look quite planar, with all the antinodes having the same amplitude. They are also contradictory in that they show antinodes for both pressure and velocity at the apex. (The velocity plots given are really those for an open pipe rather than a cone.) The discussion speaks of a mathematical singular point at the apex modifying the first *quarter*-wavelength of the standing wave, which sounds rather like the approach of White and White.

Three interesting and valid contributions are found in the books by Benade,[1,12] Strong and Plitnik,[13] and the second edition of Backus.[14] Benade stands quite apart from the others discussed here in that his attention is focused not on the simple shapes, but on the more sophisticated and complicated bores of actual instruments, particularly the hybrid bores of modern brasses. Thus we do not even find the standard pictures of standing waves in straight pipes in his books, so the seeming paradox has no opportunity to arise. Both the pipe and the cone are treated as special cases of the larger family of Bessel horns, in the spirit of the mathematical treatment to be found in Morse.[15] Strong and Plitnik approach the cone by continuous modification of a closed pipe, expanding the open end and contracting the closed end. They then use ideas that are very helpful for understanding vocal formants[16] to discuss qualitatively the shifts in the frequencies of the resonance peaks. One unique feature of their treatment is a graph of input impedance for a cone and for a cylinder of the same length, like our Fig. 5.

In the second edition of his textbook, Backus considers a sequence of open, truncated cones, starting with an open pipe and ending with a complete cone, all of the same slant length. By following the reflections of a pulse wave, he argues that the modal frequencies remain constant throughout the sequence. The limit of the complete cone is troublesome for this approach and leads to the apparently self-contradictory statement that "although the displacement is zero at the tip, the shape of the displacement impulse is so changed on reflection that it looks as if it had been reflected from an open end." Backus also argues (correctly but unconvincingly) that this type of analysis would not work for a truncated cone closed at its small end; that is easy to see from the nonharmonicity of the modal frequencies, but not from his description of a pulse reflecting off the closed end. There are several erroneous claims here regarding the nature of the distortions to a displacement pulse and the reflection of a pressure pulse at the small end. Backus concludes with accurate plots of the first three standing waves in a complete cone, shown both as pressure and as displacement. (These are also given in Hall[4] and Rossing.[5]) In his discussion of them, he again describes the tip as reflecting "like an open end," even though his figures seem to contradict that description.

III. THE FORMAL MATHEMATICS

Our overall goal in this paper is to achieve a physically correct understanding of the conical bore, the essence of which can be expressed in words and pictures. (Some of would even maintain that it is unwise to venture into the mathematical details without first laying down such an intuitive foundation.) This section is included for those who feel more comfortable with differential equations and boundary-value problems. The general problem we consider could be valuable as an exercise for physics majors who are just becoming familiar with this area; while it formally requires "spherical Bessel functions of order zero," in fact the solutions can be obtained by thinking only in terms of sinusoids.

A. Spherically symmetric waves

We begin with the linear wave equation of acoustics:

$$\nabla^2 p - c^{-2}\frac{\partial^2 p}{\partial t^2} = 0. \qquad (1)$$

Notice that this is an equation for acoustic *pressure* as a function of position and time. If we express the Laplacian operator in Cartesian coordinates, then it is apparent that this equation is also satisfied by any Cartesian component of the particle acceleration, $a_i = -\rho^{-1}\partial p/\partial x_i$. One or two time integrations will then show that any Cartesian component of the acoustic particle velocity or displacement will also satisfy this equation. Thus among the larger class of solutions to this equation in three dimensions we find the familar plane wave or one-dimensional solutions, in which pressure and particle velocity satisfy the same equation and show the same behavior.

In this work our attention is focused on solutions with spherical symmetry. For that symmetry the Laplacian takes the form

$$\nabla^2 p = r^{-2}\frac{\partial(r^2\partial p/\partial r)}{\partial r} = r^{-1}\frac{\partial^2(rp)}{\partial r^2}. \qquad (2)$$

Since $a_r = -\rho^{-1}\partial p/\partial r$, we differentiate Eq. (1) with respect to r to find the equation satisfied by a_r:

$$\nabla^2 a_r - 2r^{-2}a_r - c^{-2}\frac{\partial^2 a_r}{\partial t^2} = 0. \qquad (3)$$

Again, one or two time integrations of a_r will show that the acoustic particle velocity and displacement also satisfy this equation.

Substituting the second form for the spherically symmetric Laplacian given in Eq. (2) into Eq. (1) and then multiplying through by r yields

$$\frac{\partial^2(rp)}{\partial r^2} - c^{-2}\frac{\partial^2(rp)}{\partial t^2} = 0.$$

If we let $rp(r,t) = P(r,t)$, then we get a simple one-dimensional wave equation for P,

$$\frac{\partial^2 P}{\partial r^2} - c^{-2}\frac{\partial^2 P}{\partial t^2} = 0,$$

for which the traveling wave solutions $f(r+ct)$ and $g(r-ct)$ are well known. Thus we obtain the almost equally well-known result that

$$p(r,t) = f(r+ct)/r + g(r-ct)/r$$

is the general solution of spherical symmetry for Eq. (1). We shall call $f(r+ct)$ and $g(r-ct)$ the *permanent parts* of the inward- and outward-propagating spherical waves, because those numerators are simply translated without distortion as time progresses.

By differentiating the spherically symmetric solution for p with respect to r, we obtain the noticeably more complicated general form of the solution of Eq. (3) for the radial particle acceleration, velocity or displacement:

$$r^{-1}\frac{\partial[f(r+ct)+g(r-ct)]}{\partial r} - r^{-2}[f(r+ct)+g(r-ct)].$$

The first term of this solution has the same general form as that for p, but the presence of the second term prevents us from identifying any "permanent" behavior in the total solution. The second term clearly becomes more important as r decreases, and for that reason it is called the *nearfield* term.

Thus we have established a very unsymmetric relationship between p and $\mathbf{v}$ for the cases of interest to us. In one dimension, these two quantities are on equal footing, in that they satisfy the same equation and have the same simple form for their solutions. When we have spherical symmetry, p satisfies a noticeably simpler equation and has solutions of a noticeably simpler form than v_r does. *For that reason we shall do all our work from here on in terms of p.*

B. Waves of a specific frequency

A standard technique for solving Eq. (1) and others that can be put into a similar form is separation of variables. A particularly convenient approach is to allow complex solutions and then take their real parts at the end. The solutions of the temporal equation that is obtained on separation have the form $e^{\pm i\omega t}$, and the spatial equation then takes the form

$$\nabla^2 p(r) + \omega^2 c^{-2} p(r) = 0,$$

which is known as the Helmholtz equation.

In the case of spherical symmetry, we use the same approach as in part A to obtain $p(r) = e^{\pm ikr}/r$, where $k = \omega/c$. To avoid redundancy in our solutions when we take their real part, we shall restrict the temporal solution to the form $e^{-i\omega t}$ with $\omega > 0$. Then the $+k$ and $-k$ solutions represent, respectively, outward- and inward-traveling spherical waves. The two complex spatial functions

$$h_0^{(1)}(kr) = e^{-ikr}/kr$$

and

$$h_0^{(2)}(kr) = e^{+ikr}/kr$$

are called spherical Hankel functions or spherical Bessel functions of the third kind and zero order. The two standing wave solutions $j_0(kr) = \sin(kr)/kr$ and $n_0(kr)$ or $y_0(kr) = -\cos(kr)/kr$ that can be formed from them are called, respectively, spherical Bessel functions of the first and second kind (zero order), or else simply spherical Bessel and Neumann functions. Notice that the spherical Neumann function diverges at the origin, and for that reason, it does not really satisfy the source-free Helmholtz equation there. Instead, this implies that a point source or spatial delta function in three dimensions should appear on the right side of the equation. In many boundary-value problems, the Neumann functions are ruled out because the origin is included in the region of interest and there is no explicit source term there.

C. Open–open frustum

This is the simplest case to consider among the idealized boundary-value problems we shall examine. We imagine that somehow we are able to establish a wave impedance of exactly zero at the two open ends of a truncated cone, $r = r_1$ and $r = r_2$ in Fig. 1. This implies the boundary condition that $p = 0$ at each end. In terms of the spherical traveling wave solutions, this requires that they have equal amplitude at any point and that they be out of phase at each end. The standing wave solutions are of the form

$$p(r) = \sin[k_n(r-r_1)]/r,$$

where

$$k_n(r_2 - r_1) = n\pi,$$

or

$$f_n = k_n c/2\pi = nc/[2(r_2 - r_1)] = nc/2L,$$

with L the length of the frustum. Notice that these are the same natural frequencies as for an (idealized) open pipe of length L. The reason for this is that the denominator in the standing wave $p(r)$ does not enter into meeting the boundary condition, and the numerator has just the form of a straight pipe standing wave.

An interesting feature of this solution is the fact that we can take r_1 continuously to zero. In that limit, we no longer have an open–open frustum but now a cone complete to its apex, which of course is closed. Simultaneous with r_1 becoming zero, we find that the standing wave changes from having a node at r_1 to having an antinode there, so the new boundary condition

$$a_r|_{r=0} = -\rho^{-1}\partial p(r)/\partial r|_{r=0} = 0$$

is satisfied. This proves the claim made earlier that a cone complete to its apex has the same natural frequencies as an

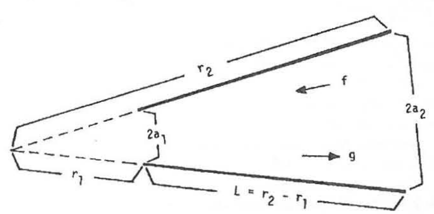

Fig. 1. Parameters used in treating the various frusta.

open pipe of the same length, even though the boundary condition at the apex is very different from that at an open end of a pipe.

If the standing wave is expressed in terms of the spherical Bessel and Neumann functions, which can be done very simply using a trigonometric identity on $\sin k(r - r_1)$, then we see that n_0 is required as part of that solution as long as $r_1 \neq 0$. In the limit as r_1 goes to 0, the coefficient multiplying n_0 goes linearly to 0, consistent with the more common boundary-value problems that include the origin in the region of interest. (The standard approach is to rule out the various Neumann functions because they all diverge at the origin. It would be more accurate to say that they are excluded because the origin is neither a source nor a sink for waves, if that is in fact the case.)

D. Closed–open frustum (small end closed)

For this geometry we will find it useful to define the parameter $B = r_1/r_2$, which is also equal to the small bore radius over the large one (see Fig. 1). The boundary condition at r_2 that $p = 0$ can be met automatically by taking a solution of the form $p(r) = \sin[k(r_2 - r)]/r$. Then applying the boundary condition that $\partial p/\partial r = 0$ at $r = r_1$ leads to

$$\tan[\pi(f/f_0)] = -(1 - B)^{-1}B\pi(f/f_0), \tag{4}$$

where $f_0 = c/[2(r_2 - r_1)]$ is the fundamental frequency for the open pipe of length $L = r_2 - r_1$ (see Fig. 2, quadrant D).

The various roots of this equation are shown as a function of B in Fig. 3 (solid curves). Notice that for small values of B, the tangent plot in Fig. 2 can be approximated as a

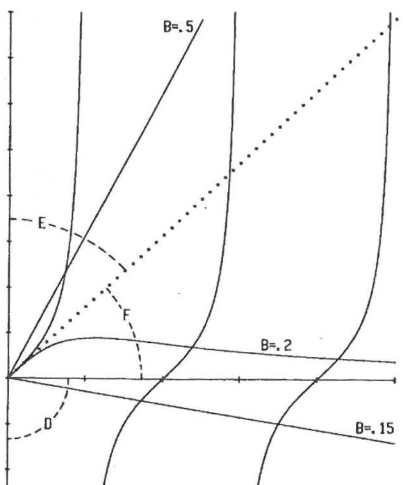

Fig. 2. Graphical solutions of the transcendental equations for the modal frequencies. Quadrant D, closed–open frustum; octant E, open–closed frustum; octant F, closed–closed frustum.

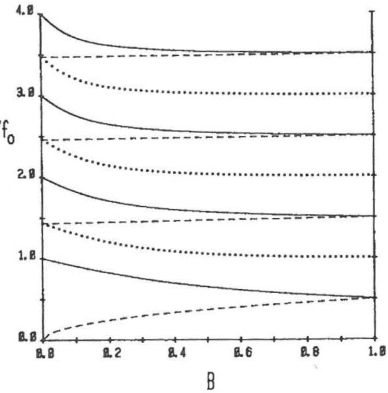

Fig. 3. Modal frequencies normalized to f_0, the fundamental for an open pipe of the same length as the frustum. Solid curve, closed–open; dashed curve, open–closed; dotted curve, closed–closed.

succession of straight lines crossing the horizontal axis, so for the nth root we find

$$f_n \cong n(1 - B)f_0 = n(1 - r_1/r_2)c/[2(r_2 - r_1)] = nc/2r_2. \tag{5}$$

The physical significance of this, which is pointed out in several musical acoustics textbooks, is that for *small* truncations, the cone closed at its small end acts almost as though it had been completed to its apex. The musical significance is that a nearly harmonic relationship among the natural frequencies (which can be improved by perturbations of this bore shape) preserves the usefulness of the slightly truncated cone, since it can then support harmonic regimes of oscillation.[1] In Fig. 3, this approximation would appear as a fan of straight lines, tangent to the solid curves at $B = 0$ and intersecting in the lower right corner.

Overall, as B increases from 0 to 1, the slope of the straight line intersecting the tangent curve in quadrant D of Fig. 2 varies smoothly from 0 to $-\infty$, and the natural frequencies drop smoothly from the harmonics of f_0 for the complete cone to the odd harmonics of $f_0/2$ for the closed pipe. For any intermediate value of B, the lower natural frequencies tend to be a bit sharp from exact harmonics of the fundamental (cone-like behavior), while the higher natural frequencies approach the odd harmonics of $f_0/2$ from above (closed pipe behavior).

E. Open–closed frustum (small end open)

The cone that is open at its small end and closed at its large end is not useful musically, but it is easy to deal with from our approach. In this case we find it convenient to return to the form of the solution assumed in part C, since that automatically meets the boundary condition that $p = 0$ at $r = r_1$. Then applying the boundary condition that $\partial p/\partial r = 0$ at $r = r_2$ leads to

$$\tan[\pi(f/f_0)] = (1 - B)^{-1}\pi(f/f_0) \tag{6}$$

with B and f_0 as defined in the previous section. (This is the same as the solution in that section with $1/B$ substituted for B. Perhaps a more elegant approach to these two cases would be to define B as the ratio of the closed end radius to the open end radius and let this parameter vary continuously from 0 to ∞. We find it more convenient in representing our results graphically to stay with our original definition.)

The interesting feature of this result is the near constancy of the higher modal frequencies while the fundamental plunges to zero as B goes to 0. The fundamental might very well be called the Helmholtz mode, because for small B the air in most of the cone acts like a massless spring, while that in the "neck" constitutes a stiff plug, just as in the Helmholtz resonator. If we take that plug to be a cylinder just fitting into the neck, its effective length is r_1. Notice that this lowest mode, which can be traced back continuously to the fundamental for the complete cone open at its large end, now disappears by dropping to zero frequency. This loss of a mode is physically reasonable, since closure of the small end of the cone (with the large end already closed) means that the air on the inside no longer communicates with that on the outside. In terms of Fig. 2, as B drops from 1 to 0, the slope of the straight line in octant E drops from ∞ to 1, and ultimately the intersection with the first branch of the tangent curve is lost.

F. Closed–closed frustum

This completely closed structure is clearly of no use as an acoustic musical instrument, since there is no way to drive it or detect its standing waves (except by electronic means). However, as a boundary-value problem, this geometry is the most interesting because we cannot meet the boundary condition at either end by a simple choice of the form for $p(r)$. If we impose the boundary conditions that $\partial p/\partial r = 0$ at both r_1 and r_2, then turning the crank on some algebra ultimately yields the transcendental equation

$$\tan[\pi(f/f_0)] = [1 + B(1-B)^{-2}(\pi f/f_0)^2]^{-1}\pi(f/f_0). \quad (7)$$

As we might expect, the solutions for this case are found in the remaining wedge of Fig. 2, the octant labeled F. However we are no longer intersecting the tangent curve with a straight line, but instead with the more complicated curve on the right side of Eq. 7. Consistent with our discussion at the end of the previous section, we find that this curve fails (just barely!) to intersect the first branch of the tangent plot.

In the limit as B goes to 1, we come back to a straight pipe, but now it is closed at both ends. We see that it has the same natural frequencies as the complete cone and hence the idealized (no end corrections) open pipe of the same length. The standing waves in those two straight pipes are just the converse of each other; while the open pipe has pressure nodes at each end, the closed one has antinodes there. If we follow the circuitous connection of these structures through parts C, D, E, and F, we see that the fundamental mode of the closed–closed pipe is actually related to the *second* mode of the open pipe, the fundamental of the latter having disappeared (by dropping to 0 Hz) when the structure became completely closed. This is entirely consistent with the more direct connection achieved by simply closing the ends of the open pipe in a continuous manner; it it well known that narrowing or partial closure of an open end drops all the natural frequencies.[13,16] Indeed, the qualitative behavior of the natural frequencies in parts D and E can be understood in terms of that principle and/or the related one to the effect that widening a closed end also drops the natural frequencies.

G. Some references

As is the case for a great many useful calculations in acoustics, we can trace the work of this third section back to Lord Rayleigh.[17] In particular, article 281 in his *Theory of Sound* deals with the open–open frustum of part C and the closed–closed frustum of part F. That work is done in terms of the velocity potential, which is equivalent to working with pressure at any one frequency; however when he discusses nodes and antinodes of the standing waves, he speaks in terms of the particle velocity.

Morse[15] covers the cone in a general discussion of horns, including those of exponential and catenoidal shape. The focus of this work is on transmission coefficients for geometries that would be suitable for loudspeakers, but the resonance frequencies of horns with small mouths are also obtained by looking at extreme values for the input impedance. Minima in that curve correspond to the open–open case of part C and maxima to the closed–open case of part D. He does not consider any structures that are closed at the large end.

Benade[18] has examined the closed–open and open–closed frusta of parts D and E as specific examples of a different general class called Bessel horns. Both Benade and Morse are solving an approximate wave equation called the "Webster" horn equation (which turns out to be exact in the case of the cone), so comparison with the present work is nontrivial. Our more direct solution for the simple, special case of the cone could be taken as one check on their results.

In addition to his purely descriptive work,[10] Taylor has also previously written a book on musical acoustics that would be suitable for upper division physics majors,[19] since it goes into the differential equations involved. He obtains the natural frequencies for a cone complete to its apex, first with the large end open and then with it closed. The style of his calculation is along the lines of Rayleigh and this paper. In light of this careful work, we find it surprising that this author could come up with the explanation in his descriptive book.

IV. THE STANDING WAVES

Often in solving boundary-value problems, we heave a sigh of relief on obtaining the eigenvalues and move on to other work, but even if we have no explicit need for the eigenfunctions, it can be quite instructive to examine them for an explanation of the behavior of the eigenvalues. This extra effort is particularly worthwhile in the present case because of the simple form for the pressure standing waves.

Perhaps a bit surprisingly, it is also at this point that we can bring the students in a descriptive course in on our attempts at a physically correct, intuitive understanding of the major results. Almost all of the books discussed in Sec. II include the necessary background material for developing spherical waves: the inverse square law for the sound intensity from a point source and the proportionality of intensity to the square of the pressure amplitude. A little proportional reasoning then shows that a sinusoidal point source puts out a spherical traveling wave whose amplitude varies inversely with distance from the source. If that wave is reflected from a spherical barrier centered on the source, then the reflected wave shows the same $1/r$ strengthening as it converges back upon the source. The two traveling waves interfere to give a spherical standing wave whose *pressure nodes* are separated by the *normal half-wavelength spacing*, but with a $1/r$ factor governing the overall behavior of its amplitude. Notice that any "distortion" of such a pressure standing wave compared to the sinusoidal shape that we see in a one-dimensional situation is in the *amplitude only*. (The same cannot be said for the radial component of velocity or displacement, which can be found by taking the gradient of the pressure and integrating once or twice in time.)

We now tailor the general three-dimensional solution to fit the sequence of four different bores shown in Fig. 4. The values of B for the four cases shown here are 1, 1/4, 1/20, and 0, from top to bottom. In our plots of the standing waves, we employ the usual idealizations that the nodes are locations of complete cancellation of the acoustic pressure in the two traveling waves and that such nodes are found exactly at the open ends.

A. Open–open frustum

It is clear from the figures that in the first three frusta, the wavelength is unchanged from that for the open pipe of the same length as the slant length of the frustum. The progressively stronger distortion of the amplitude by the $1/r$ spherical factor as the apex approaches the left end is also quite clear. If reference to the (virtual) apex strikes the students in a descriptive course as a little too abstract, one can instead define that factor as the reciprocal of the local bore diameter. However, we must then be careful not to imply that the wavelength arguments carry over to bores with other shapes. (The enhancement of acoustic pressure with decreasing bore diameter can be demonstrated quite easily using a cone of large half-angle as an old-fashioned "ear trumpet" type hearing aid.)

Each standing wave for the complete cone shown at the bottom of Fig. 4 should be thought of as the limit for the sequence above it as the left end of the cone finally closes. Notice that we do not get into any contradictions here. As long as the left end is open, it is the location of a pressure node, and for the very same step in which it closes, that node is replaced by an antinode. The sequence of figures shows how this happens: the leftmost antinode continuously increases in strength and approaches the left end until it simply "runs over" the node that was there.

The important thing to notice in this sequence of closing the cone from the original open pipe is that throughout the whole process, including the last step, the wavelength and hence the frequency for each mode have stayed the same. Notice in particular the fixed locations of the pressure nodes. Our claim that the whole fundamental standing wave for the complete cone (and the similar portion of its higher modes) is actually a half-wavelength rather than quarter-wavelength may be a little hard to accept at first. However, examination of the explicit functional dependence—$(\sin \pi L^{-1} r)/r$—reminds us that we have seen this plot before, perhaps as the diffracted amplitude due to a single slit (with the central lobe twice as wide as the others), or perhaps as the well-known sinc function of Fourier transforms, or else as the spherical Bessel function j_0, which is exactly the role that it is playing here. Students in a descriptive course will not know about l'Hopital's rule, but they can accept the idea that zero times infinity might be zero or infinity or, as this case, a finite value.

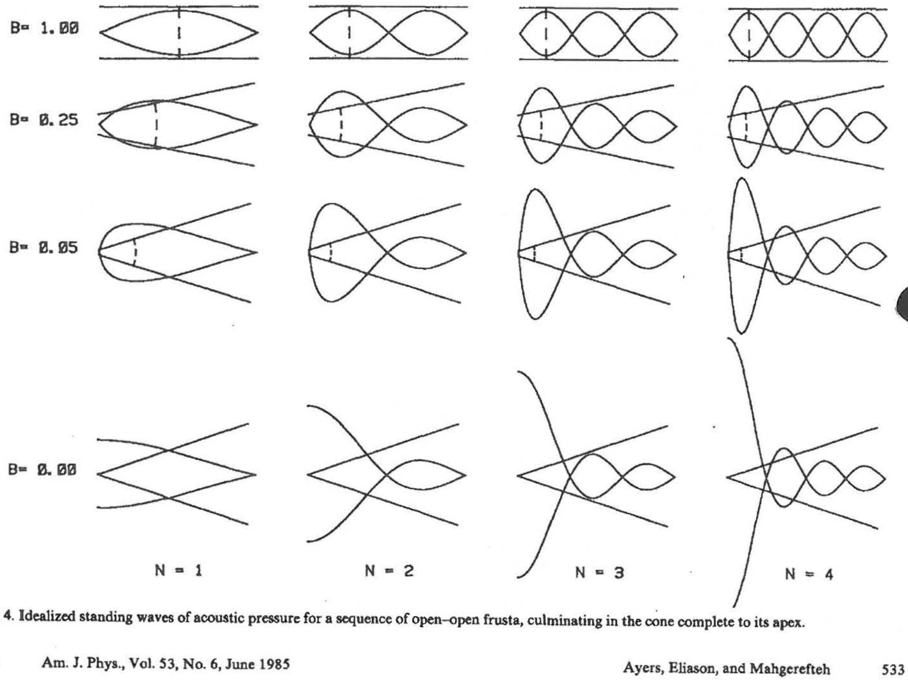

Fig. 4. Idealized standing waves of acoustic pressure for a sequence of open–open frusta, culminating in the cone complete to its apex.

B. Closed–open frustum (small end closed)

The dashed arcs in Fig. 4 locate the leftmost pressure antinode and displacement node in each standing wave of the truncated cones and the straight pipe. If we discard the portion of the bore and standing wave to the left of this location, then we have a standing wave for a closed, shortened bore but with the same half-wavelength and mode number as before. Expressing that new bore length in terms of the half-wavelength then gives us the ratio of this mode's frequency to f_0, the fundamental for an open pipe or complete cone of the same length. For example, examination of the top figure in each column yields the familar results that $f_1/f_0 = 1/2$, $f_2/f_0 = 3/2$, $f_3/f_0 = 5/2$, and $f_4/f_0 = 7/2$ for the closed pipe.

The cases intermediate between the closed pipe and the complete cone are not so easy to handle. For the students in a descriptive course, we can locate the antinodes graphically and determine f_n/f_0 using the shortened bore lengths. However, we must recognize that with the additional truncation, the bore ratio B is also increased, and by different amounts for different modes. Perhaps the best we can do for these students is to present the curves for this geometry shown in Fig. 3, point out that the change from the cone on the left to the closed pipe on the right is continuous, and locate the eight specific points that correspond to the intermediate cases of Fig. 4.

C. Open–closed frustum (large end closed)

The relevant standing waves can be seen in Fig. 4 by locating the *rightmost* pressure antinode and discarding the bore and standing wave to the right of it. The very small shift in location of that antinode for the second and higher modes shows that their frequencies will hardly vary. The fundamental frequency, on the other hand, will vary dramatically, dropping to zero as the small end closes.

D. Closed–closed frustum

For this geometry, just retain that portion of each standing wave between its two outermost pressure antinodes. Notice that there is no such portion for the left column. This is consistent with the disappearance of the Helmholtz mode on completely closing the structure and means that we must shift the mode numbers one column to the right.

V. INPUT IMPEDANCE CURVES

Our discussion so far has dealt only with the modal frequencies of conical bores for specific boundary conditions at the two ends. A more general quantity that is useful to examine is the input acoustic impedance, defined as the ratio of pressure amplitude to volume velocity amplitude (area times particle velocity amplitude), measured at the input end. This input impedance measurement does not impose any specific boundary condition on the input end; a plot of its dependence on frequency yields the modal frequencies for the bore with its input end closed at maxima and those for the bore open at its input end at minima (except for the effect of a missing end correction at the input end).

Figure 5 shows experimental plots of input impedance for a straight pipe and a nearly complete cone ($B = 0.20$), each open at the far end. Their effective lengths for low

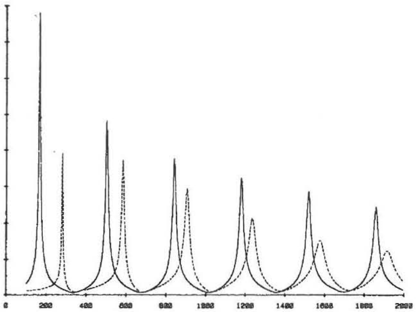

Fig. 5. Input impedance curves for a straight pipe (solid) and a frustum (broken) of the same effective length.

frequencies are approximately equal at about 50 cm. The data were obtained by the capillary excitation technique,[20] using apparatus designed by one of us (L.J.E.) which will be described in a separate article.[21] The shapes of these curves can be understood quite easily in terms of the standing wave plots. As the frequency is increased from zero, the wavelength decreases, but the standing wave must always have a pressure node at the open, output end of the bore. In the process of shrinking the wavelength, whenever a new pressure antinode passes through the input end, the input impedance hits a maximum. Similarly, a new pressure node passing through the input end gives rise to an impedance minimum.

The regular spacing of nodes and antinodes in planar standing waves gives rise to the regular sequence of impedance extrema for the straight pipe, with the maxima falling midway between the minima. The fact that the location of a pressure node is not influenced by the $1/r$ spherical amplitude factor explains the stability of the impedance minima when the straight pipe is distorted into a cone. (The slight deviations visible at higher frequencies are due to the fact that the open-end correction at the large open end of the cone is decreasing there.[22]) On the other hand, a pressure *antinode* is shifted away from the large end by the $1/r$ factor, requiring a higher frequency for the cone than for the pipe to place it at the input end and generate an impedance maximum. The small value of B used here assures that each impedance maximum is shoved fairly close to its upper limit—the fixed minimum above it.

Fletcher[11] and Taylor[10] both claim that there is no difference between an open apex and a closed apex, in Fletcher's argument because of the mathematical singularity there and in Taylor's (erroneously) because everything is damped out there. We see now that a less abstract and more physically relevant statement is that, as the cone approaches completeness, the maxima and minima of input impedance *seen from the small end* become negligibly different *in their frequencies*.

VI. IMPULSE ANALYSIS

Backus's pedagogical discussion in terms of a pulse wave[14] works fine for truncated cones that are open at the small end, but it gets into trouble with the complete cone. The difficulty arises out of failure to distinguish between the pulse and what we have called its *permanent part* in Sec.

IIIA, the numerator $f(r \pm ct)$ of the general form $f(r \pm ct)/r$. Closure at the apex clearly calls for a velocity node and hence a pressure antinode there. We might expect to meet that boundary condition with a simple, *non*inverting reflection of the permanent part, but it is the sum of the two *pulses* (including their diverging $1/r$ factors) which must satisfy the boundary condition. This is achieved with a simple *inversion* in sign of the permanent part. Then the zero value and vanishing second derivative for the sum of the permanent parts at the apex guarantee a finite pressure with zero gradient there by l'Hopital's rule.

The case of the frustum closed at its small end presents another difficulty for the pulse discussion. It is clear from the nonharmonic relationships among the modal frequencies found earlier that there must be distortion of the pulse on reflection which cannot be undone by later reflections; otherwise there would be some period for the pulse's overall motion, implying harmonic modal frequencies. The idealized reflections from an open end of a bore or the closed end of a straight pipe are both reversible distortions in that another reflection from the same type of end completely undoes the first distortion. The distortion upon reflection at the apex of a cone is the same as for an open end. This explains the harmonicity of the modal frequencies for the closed pipe, the open pipe, the open frustum, the complete cone, and the pipe closed at both ends, the first of these requiring two round trips for a fundamental period, the others only one.

In the frustum closed at its small end, the only candidate for a nonreversible distortion of the pulse is the reflection at the closed end. Unfortunately, the distortion there as described by Backus is quite reversible, and the same as for a closed end of a straight pipe. He also implies that there will now be a nonreversible distortion at the open end, while that was supposedly not the case when both ends of the frustum were open.

The actual distortion at the closed end can be found by expressing the boundary condition there in terms of the permanent parts of the two pulse waves, Fourier transforming that relationship, solving for a transfer function, and inverse transforming to find the impulse response for the reflection.[23] In doing this work, we find it convenient to set up an origin of coordinates at the closed end, where $r = r_1$, so that $\alpha = r - r_1$ and the incoming wave has the form $f(t + \alpha/c)/r$. The most convenient expression for the reflected wave has the form $g(t - \alpha/c)/r$. The result of this calculation tells us that for any incoming permanent part $f(t)$, the reflected permanent part $g(t)$ is obtained by convolving $f(t)$ with the impulse response

$$I_3(t) = \delta(t) - 2t_1^{-1} e^{-|t/t_1|} H(t), \tag{8}$$

where $\delta(t)$ is the Dirac delta function, $H(t)$ is the Heaviside step function, and $t_1 = r_1/c$.

This interesting form shows that the reflected permanent part includes a mirror image identical with that for the closed end of a straight pipe [from the $\delta(t)$ term] plus an additional term that gives it an inverted, exponentially decaying "wake," which is certainly a nonreversible distortion. In the limit as r_1 goes to infinity for the straight pipe, we see that the wake term has infinite length and zero strength, so we recover the correct behavior. In the other limit, as r_1 goes to zero for the complete cone, the wake term becomes a delta function of strength -2 at the origin, neatly cancelling the straight pipe term and leaving the net $-\delta(t)$ that we need for the inverted reflection in that case.

The transfer function, which represents the filtering action of the reflection as a function of frequency, is just the Fourier transform of the impulse response. Its very simple form,

$$T_3(\omega) = -(1 - j\omega t_1)/(1 + j\omega t_1) = e^{j\phi},$$

where $\phi = \pi - 2\arctan(\omega t_1)$, shows that the nature of the distortion on reflection is merely a varying phase shift for the different Fourier components of the permanent part.[24] The low-frequency limit of that shift is π, and the high-frequency limit is 0. In the limit of the complete cone, t_1 goes to zero and all frequencies look "low," while the straight pipe limit has t_1 going to infinity and all the frequencies look "high." Thus we obtain the two extreme limits of simple inversion or noninversion on reflection, neither of which distorts the permanent part.

To display the behavior for intermediate values of t_1, we have convolved the impulse response for several values of [illegible] with an input pulse of finite width whose permanent part is one period of a raised, inverted cosine curve (a Hanning pulse):

$$f(t) = \Pi(t/T - 1/2)[1 - \cos(2\pi t/T)]/2$$

(see Fig. 6). Here the symbol $\Pi(x)$ stands for the rectangle function, defined as having value 1 for $|x| < 1/2$ and value zero otherwise. These curves show a smooth transition between the two extremes. For small values of t_1 as the reflected pulse becomes almost perfectly inverted, we find that it is delayed relative to the incident one by $2t_1$, the time for the round trip on to the (virtual) apex and back. Thus we again find the slightly truncated cone acting as if it were completed to its apex, as was pointed out in the discussion of Eqs. (4) and (5).

Our discussion so far has been concerned only with pulses reflected at the truncated end of the cone. If we also require that f and g be related by a simple inversion at the open end [i.e., that $f(t + L/c) = -g(t - L/c)$], we obtain exactly the same transcendental equation for the natural frequencies as before [Eq. (4)]. When the cone is complete, corresponding to $t_1 = 0$, an impulse incident on the apex is

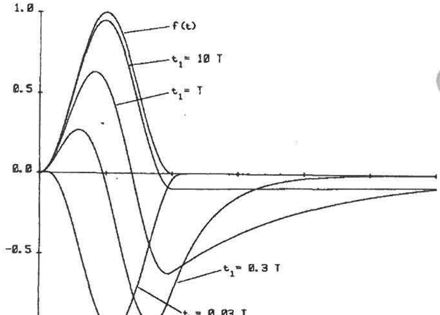

Fig. 6. Reflections of a Hanning pulse from the closed small end of a cone for different values of $t_1 = r_1/c$.

reflected with a simple inversion and the natural frequencies are harmonically related. But when the cone is truncated, the waves associated with each reflection at the closed end successively degrade the pulse and introduce nonreversible distortion. Such distortion prevents a return to the original pulse shape and thus prevents periodic behavior. Since periodic behavior occurs if and only if the natural frequencies are related harmonically, we see that the presence of the wake corresponds to the existence of nonharmonic natural frequencies.

Before we show how the shape of a pulse is changed by a succession of reflections, let us describe the input pressure pulses with which we will be working. In our experimental system, the input at the small end of the cone is a *volume velocity* pulse rather than a pressure pulse. The pressure impulse response to a volume velocity impulse as input is

$$p(t) = \rho c S_1^{-1} I_1(t),$$

where

$$I_1(t) = \delta(t) - t_1^{-1} e^{-|t/t_1|} H(t).$$

(S_1 is the cross-section area of the bore at the input end.) We obtained this result using the same approach as for I_3, but with the boundary condition that at $r = r_1$,

$$-\nabla p = \rho \frac{\partial v}{\partial t};$$

it is also given by Morse.[15] Notice that relative to the $\delta(t)$, the wake here is only half as strong as that for $I_3(t)$ given in Eq. (8). The next figure (Fig. 7) shows the effect of several reflections of a pulse. Curve v shows the volume velocity input, a Hanning pulse that approximates the input of our experimental system. (This is the same function as that used for the input pressure pulse in the previous figure.) Curve e shows the resultant outgoing pressure pulse. Assuming that an outgoing pulse is eventually changed to an incoming pulse as the result of a simple reflection *without* inversion, curves g_1, g_2, and g_3 show the results of sequential reflections at the truncated end of the cone. The progressive changes in the pulse shape are quite clear.

We have observed multiple reflections experimentally in a closed–open frustum. In order to display f and g separately, we placed the microphone near the middle of the frustum. A velocity pulse generated at the small end using a small piezoelectric transducer[25] gave rise to a pressure pulse which was then reflected repeatedly at each end. The first segment of the upper curve in Fig. 8 shows the pressure at the middle of the cone as the pulse produced at the small end moves past the microphone toward the large end. The following segments show the pulse after sequential reflections at the large and small ends. As predicted by the analysis, the wake is present in the first pulse and is modified by the sequential reflections. The fine structure that is especially prominent in the early segments is due to ringing in the transducer.

We have calculated the extended impulse response of our system for a Hanning pulse volume velocity input under the assumptions that (a) only a simple inverting reflection with a slight loss occurs at the far end [$I_2 = -d_2\delta(t)$ with $d_2 < 1$], and (b) there is another constant-amplitude loss factor upon each reflection at the near end (actually arising from damping in propagation as well as the finite stiffness of the transducer closing the small end). The result is shown in the lower curve.

If we were to shift the microphone gradually along the frustum until it reached the small end, we would see the succession of incoming reflections f_n shifting later in time until each f_n overlapped the corresponding g_n, with their leading edges coinciding. At that point, we would have the extended impulse response whose Fourier transform was simply the input impedance curve for the cone shown in Fig. 5.

VII. CONCLUSIONS

The cone is a geometrically simple structure that shows acoustically simple behavior, with harmonic natural frequencies. In order to establish the connection between structure and behavior as clearly as possible, we found that we had to abandon the variables almost universally favored in lower division textbooks and focus on the simpler behavior of the acoustic pressure. The traditional prejudice in favor of particle velocity or displacement could perhaps be argued on the basis that these are somehow less "abstract" quantities, at least conceptually and for beginning stu-

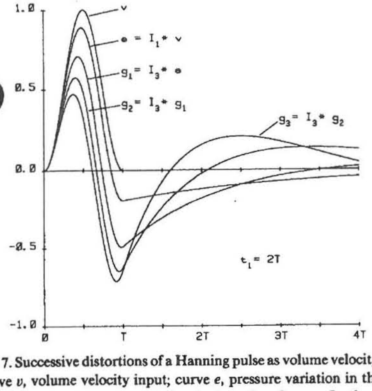

Fig. 7. Successive distortions of a Hanning pulse as volume velocity input. Curve v, volume velocity input; curve e, pressure variation in the input pulse; curves g_n, pressure variation in the pulse after n reflections at the closed small end of the cone.

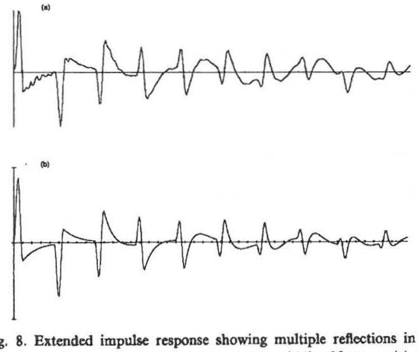

Fig. 8. Extended impulse response showing multiple reflections in a closed–open frustum; microphone located near middle of frustum: (a) experimental, (b) calculated.

dents. However, anyone who performs even the simplest of experiments with acoustic standing waves quickly realizes that it is pressure to which ears and the vast majority of microphones respond. At the input end of most wind instruments, it is the pressure variations which provide the feedback control to the driver. The manipulation of standing waves in a bore by establishing contact with open air at the end of the bell or an open side hole is most easily interpreted in terms of the pressure nodes created there.

Probably the most desirable state of affairs is to be able to describe a situation in terms of *either* pressure or particle velocity, and to move back and forth easily between the two descriptions according to whichever is the most convenient at the time. (This is somewhat analogous to using the alternative time- and frequency-domain descriptions, which are connected by the bridge of the Fourier transform.) There are of course the more sophisticated concepts of acoustic impedance and velocity potential, but these are also noticeably more abstract. We believe that the present work makes a good argument for putting pressure on at least equal footing with velocity or displacement.

Devoting this much attention to such a simple structure as the cone may seem inappropriate, but unfortunately, we find that the confusion about its behavior is not limited to descriptive textbooks. We have found some significant errors in the research literature,[26–28] and these articles are being cited by other authors. The cone is an important structure in itself, serving as the basis for so many practical instruments because it is one of the few bore shapes that have all their first several resonances lined up in a harmonic series. In calculations for larger classes of horns,[15,18] we have seen the cone fall out as a special case. It also serves as the basic element for a careful theoretical analysis of horns with nonuniform flare.[29,30] If we have a solid, physically correct understanding of the cone, then we can use that as a basis for interpretation of the results in these mathematically more complicated cases. It is our hope that this paper has contributed to an increase in that understanding.

ACKNOWLEDGMENTS

We would like to thank David M. Brown and Siamak Katal for their contributions to this work and to the ongoing project of which it is a part. Conversations with Bruce L. Scott have been very stimulating and helpful. One of us (R.D.A.) has received considerable support from California State University, Long Beach and its School of Natural Sciences in the form of released time from teaching duties and generous equipment funds. We would also like to thank Arthur H. Benade of Case-Western Reserve University for his comments on a preliminary version of this paper.

[a] Present address: Department of Physics, University of Southern California, Los Angeles, CA 90007.

[1] A. H. Benade, *The Fundamentals of Musical Acoustics* (Oxford University, London, 1976).
[2] J. Backus, *The Acoustical Foundations of Music* (Norton, New York, 1969), 1st ed.
[3] J. G. Roederer, *The Physics and Psychophysics of Music* (Springer, Berlin, 1975), 2nd ed.
[4] D. E. Hall, *Musical Acoustics: An Introduction* (Wadsworth, Belmont, CA, 1980).
[5] T. D. Rossing, *The Science of Sound* (Addison-Wesley, Reading, MA, 1982).
[6] J. S. Rigden, *Physics and the Sound of Music* (Wiley, New York, 1977).
[7] J. Askill, *Physics of Musical Sounds* (Van Nostrand, New York, 1979).
[8] R. E. Berg and D. G. Stork, *The Physics of Sound* (Prentice-Hall, Englewood Cliffs, NJ, 1982).
[9] H. E. White and D. E. White, *Physics and Music* (Saunders, Philadelphia, 1980).
[10] C. A. Taylor, *Sounds of Music* (Scribner's, New York, 1976).
[11] N. H. Fletcher, *Physics and Music* (Heinemann Educational, Victoria, Australia, 1976).
[12] A. H. Benade, *Horns, Strings and Harmony* (Doubleday, Garden City, NY, 1960).
[13] W. J. Strong and G. R. Plitnik, *Music, Speech and High Fideli*[illegible] (Brigham Young University, Provo, UT, 1977).
[14] J. Backus, *The Acoustical Foundations of Music* (Norton, New York, 1977), 2nd ed.
[15] P. M. Morse, *Vibration and Sound* (AIP, for the Acoust. Soc. Am., 1981; republication from McGraw-Hill, New York, 1948), 2nd ed., pp. 265–288.
[16] J. Sundberg, Sci. Am. **236** (3), 82–91 (March 1977).
[17] J. W. S. Rayleigh, *The Theory of Sound* (Dover, New York, 1945), 2nd ed., pp. 104–115.
[18] A. H. Benade, J. Acoust. Soc. Am. **31**, 137–146 (1959); reprinted with an erratum in *Musical Acoustics; Piano and Wind Instruments*, edited by Earle L. Kent (Dowden, Hutchinson and Ross, Stroudsburg, PA, 1977).
[19] C. A. Taylor, *The Physics of Musical Sounds* (American Elsevier, New York, 1965), pp. 26–29.
[20] J. Backus, J. Acoust. Soc. Am. **56**, 1266–1279 (1974).
[21] L. J. Eliason, to be published.
[22] H. Levine and J. Schwinger, Phys. Rev. **73**, 383–406 (1948).
[23] R. N. Bracewell, *The Fourier Transform and Its Applications* (McGraw-Hill, New York, 1978), 2nd ed. See Chap. 9 in particular.
[24] Our use of the symbol "j" in a physics journal may seem a bit strange, particularly since we have already used "i" earlier. The reason for this is that we take the Fourier transform as our principal conceptual tool, and we always require a positive sign in the exponent for the synthesis integral (inverse transform). When we are concerned with the spatial dependence of waves, as in the first part of this paper, we perform spatial transforms using the convention that is standard for physics. When we focus on signals at specific points, we perform temporal transforms using the convention that engineers prefer. Translation between these conventions is accomplished very simply by the substitution $j = -i$.
[25] M. I. Ibisi and A. H. Benade, J. Acoust. Soc. Am. **72** (Suppl. 1), S63 (1982).
[26] A. E. Bate and E. T. Wilson, Philos. Mag. **26**, 752–757 (1938).
[27] T. H. Long, J. Acoust. Soc. Am. **19**, 892–901 (1947); reprinted in t[illegible] same volume as Ref. 18.
[28] T. H. Long, J. Acoust. Soc. Am. **20**, 875–876 (L) (1948); reprinted in the same volume as Ref. 18.
[29] A. H. Benade and E. V. Jansson, Acoustica **31**, 80–98 (1974); reprinted in the same volume as Ref. 18.
[30] R. Caussé, J. Kergomard, and X. Lurton, J. Acoust. Soc. Am. **75**, 241–254 (1984).